4. Raman Spectroscopy

Raman spectrum results from transitions between vibrational states of the molecule. Molecular vibrations are complicated motions of every atom in complex molecules. Nonlinear molecules with N atoms have 3N-6 degrees of freedom giving the number of ways, in which the molecule can vibrate, i.e. the number of vibrational normal modes. Every vibration of a given molecule is characterized by a discrete set of energies. Any modification in the structure or in the environment of the molecule causes changes in the energies of the vibrations. These perturbations to the vibrational normal modes can be studied by means of Raman spectroscopy.

In this paragraph, several aspects of Raman spectroscopy are described. Chapter starts with basic introductory details of Raman effect and then continues with description of applied Raman spectrometer arrangement and measurement procedure. After that, the details of how to prepare the spectra presented in Chapter 5 from the raw collected Raman spectra are given. Finally, Raman spectroscopy of proteins, nucleic acids, and their complexes is introduced.

4.1. Raman Effect

In Raman spectrometry, the molecule is illuminated by a monochromatic source of light (laser beam). The photons of the incident radiation with frequency ν_0 interact with the molecule and raise the potential energy of the molecule to a virtual state, $h\nu_0$, above the ground state. Almost immediately the molecule returns to the ground state by emission of a photon of the same energy as incident photon. This process is called Rayleigh scattering and belongs to a class of elastic scattering because the wavelengths of incident and emitted photons are identical. In some cases, the molecule drops back to the first exited vibrational state of the n-th vibrational mode and emits a photon with different energy, $h(\nu_n–\nu_{vib})$. Since the energies of incident and scattered photons are different, the scattering is called inelastic and the process is known as Stokes Raman scattering.

Molecules that are already in excited vibrational states when illuminated will undergo analogous effects as described above. Most of the photons will be scattered with identical energy (Rayleigh scattering), but some molecules will return to the ground state of the n-th

vibrational mode and the energy of the scattered photons will be increased, $h(\nu_n+\nu_{vib})$. This effect is known as anti-Stokes Raman scattering (Figure 4.1).

In other words, the Raman effect is a light scattering process caused by transitions between vibrational states of energies E_1 and E_2. During the process a molecule absorbs the incident light of energy $h\nu_0$ ($\nu_0 > |E_2 - E_1| / h$) and immediately emits the photon ν_R, that has the energy defined by equation 1.1:

$$h\nu_R = h\nu_0 \pm (E_2 - E_1) \qquad (1.1)$$

The plus sign corresponds to the anti-Stokes scattering (Figure 4.1), in which the energy of emitted (scattered) light is increased in comparison with incident radiation, whereas the minus sign indicates Stokes scattering and the energy of emitted light is reduced. The distance between Rayleigh scattered photons ν_R and Raman scattered ones ν_0 given in wavenumbers is a property of the vibrational entity and therefore always identical and not dependent of the incident radiation frequency. Wavenumber $\tilde{\nu}$ is defined as $\tilde{\nu} = 1/\nu$. Raman scattering occurs in a time scale of 10^{-15} or less seconds and in comparison with other effects (e.g. fluorescence), the process can be considered as very fast. Figure 4.1 includes the schematical presentation of several forms of the Raman effect (preresonance, resonance, and classical) and other possible transitions in the molecule (IR, fluorescence).

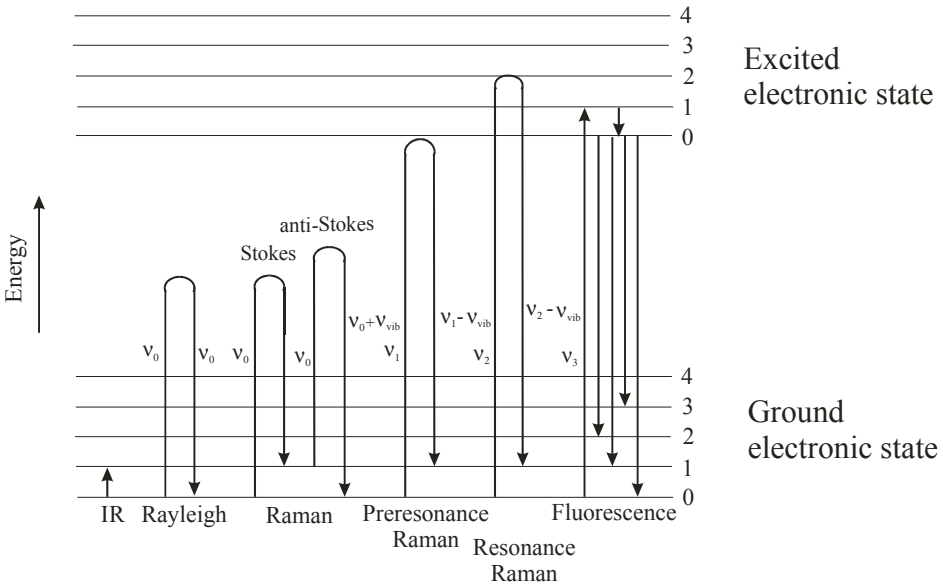

Figure 4.1: Possible interactions of incident radiation with a molecule. The length of the line heading upwards is related to the frequency of absorbed light and the line heading downwards marked with an arrow is related to the emitted radiation. The difference between vibrational states 0 and 1 is marked ν_{vib}.

If the molecule is exposed to the incident radiation (electromagnetic field), then because of different charges of electrons and protons, the negatively charged electron cloud is deformed or displaced to induce an electric dipole moment μ ($\vec{\mu} = \alpha\vec{E}$) where E is electric field vector and α polarizability. The polarizability can be regarded as the measure of the flexibility of an electron cloud. Under such conditions, the dipole moment μ_k generated in the molecule can be described as:

$$\mu_k = \alpha_0 E_0 \cos(2\pi\nu_0 t) + \frac{1}{2}\left(\frac{\partial\alpha}{\partial q_k}\right)_0 q_k^0 E_0 \{\cos[2\pi(\nu_0 - \nu_k)t] + \cos[2\pi(\nu_0 + \nu_k)t]\} \quad (1.2)$$

where q_k corresponds to the normal coordinates, ν_0 is frequency of incident radiation, ν_k is frequency of some vibrational motion of the molecule. The first term of the equation describes Rayleigh scattering, whereas the second and third term account for Stokes and anti-Stokes Raman scattering, respectively. According to equation 1.2, a given normal vibration will be Raman active and cause a band in the Raman spectrum if the vibrational motion characterized by a change in the normal coordinate q_k perturbs the polarizability of the molecule:

$$\left(\frac{\partial\alpha}{\partial q_k}\right)_0 \neq 0 \quad (1.3)$$

Further details can be found in ref 76 and 77.

4.2. Raman Spectrometer

The Raman spectrometer T64000 (Jobin Yvon, Paris, France) is a triple-spectrograph system. It contains integrated Software and Hardware package, which provides the control of the whole system and enables to set specific measurement conditions. The spectrometer is equipped with three monochromators, two detectors and two sample chambers (Figure 4.2). Laser radiation can be reflected either to the micro-chamber (microscope) or to the macro-chamber. In the Olympus BH2 microscope (Olympus, Tokyo, Japan), the scattered light is collected in 180° geometry. It means that the light is collected from the same direction as it comes. In the macro-chamber, Raman scattered light is collected in the 90° geometry (perpendicular to the illuminating radiation) to have optimal signal on the detector.

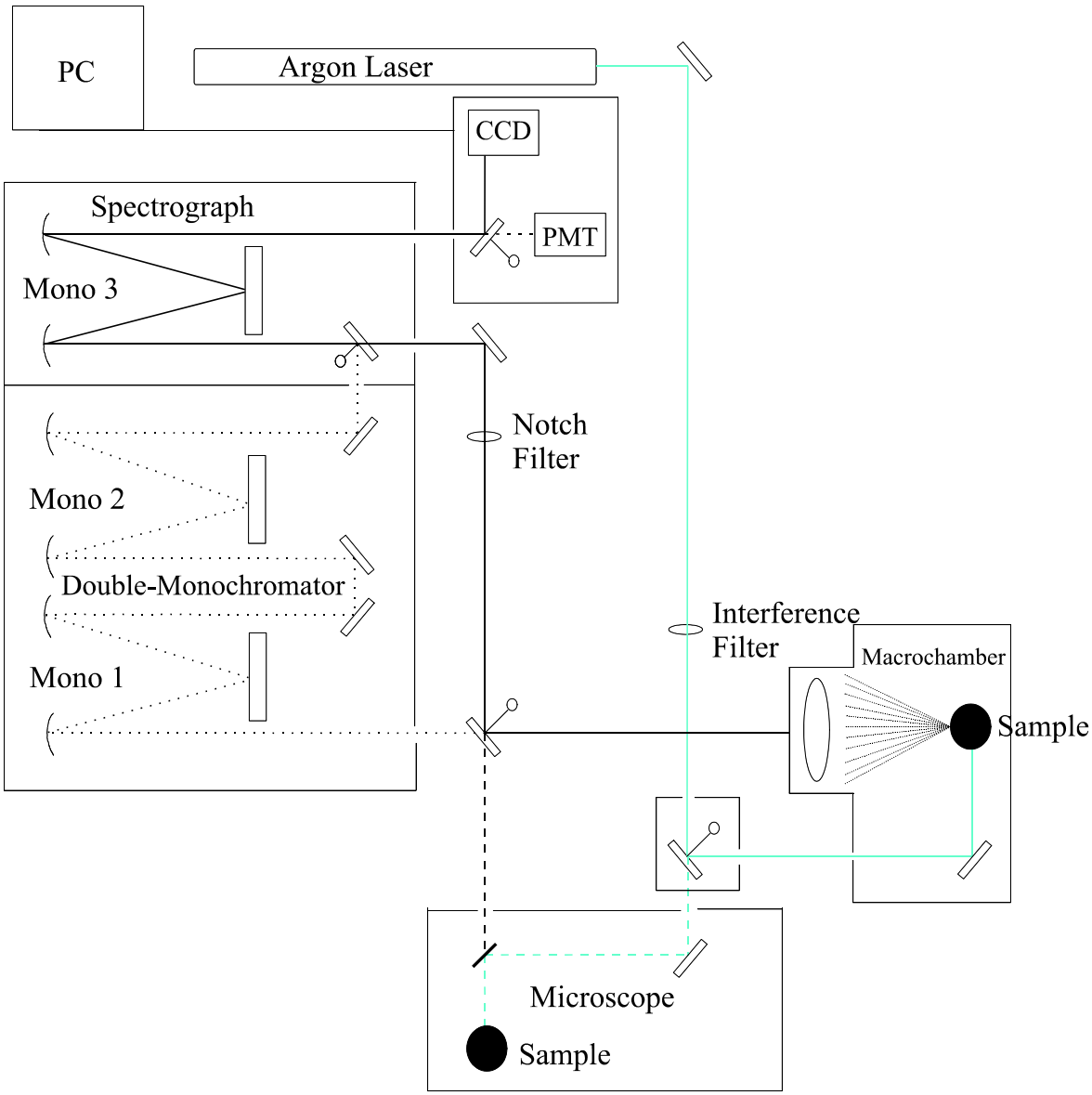

Figure 4.2: Diagram of the laser Raman spectrometer T64000. Pathway used for the collection of the Raman scattered radiation is illustrated by black solid line.

The Raman effect is very weak. Approximately, one of 10^5 Rayleigh scattered photons is Raman scattered. Intensity sufficient for precise measurements of the scattered light demands a high power of the incident radiation as achievable by a laser source. Raman spectra were obtained by employing 488 nm excitation by an argon laser Coherent Innova 90 (Coherent, Santa Clara, CA, USA). The emitted laser beam passes first through the interference filter (L.O.T. Oriel, Langenberg, Germany) that removes plasma lines and then is focused to the sample space. The radiation power at the sample in the macro-chamber was usually set to 100 mW. After that, the scattered light was collected by an objective and focused on the entrance slit of the monochromator. A notch filter (Kaiser Optical Systems, Michigan, USA) was placed between objective and entrance slit to

maximally eliminate Rayleigh scattered light. Inside the monochromator, grating with 1800 grooves per millimeter was used to disperse the Raman scattered photons on the charge-coupled-device (CCD). Finally, the nitrogen-cooled CCD detector with 298x1152 pixels (Spectraview 2-D, Jobin Yvon) connected with control unit and computer was used to visualize the signal. The working temperature of the CCD detector was ~145 K.

4.3. Spectra Measurements

4.3.1. Raman spectra

For the analysis it is essential to collect spectra with very low signal-to-noise ratio and highest possible resolution. To ensure the identical conditions for all measured spectra the following requirements had to be satisfied:

Filling of the Cuvette. Sample solutions of approximately 15 µl were filled in a homemade 15 mm long cuvette consisting of cylindrical quartz bodies with quartz bottom windows. Then, the cuvette was centrifuged for 1 min to remove air bubbles from the solution. After that, the cuvette was tightly closed with a Teflon stopper and positioned in the macro-chamber to gain the maximal signal on the CCD. Measurements were performed at stable room temperature of 22°C.

Monochromator and Measurement Region. The entrance slit dimensions of the monochromator were always set to 25 mm x 100 µm. The broadness of the entrance slit specifies the spectral resolution. Narrowing the slit would increase the resolution but reduce the intensity. The chosen settings are a reasonable compromise between resolution and intensity.

The T64000 spectrometer enables the use of two types of gratings. The first one has 900 grooves per mm and the second one 1800 grooves per mm. With the 900 grooves grating one could measure in the region from 300 to 1800 $cm^{-1}$with a low resolution not better than 1.3 cm^{-1}. In standard measurements, the grating with 1800 grooves per mm was used to achieve a spectral resolution of approximately 0.5 cm^{-1}. With this setting the CCD chip covers only 600 cm^{-1}, therefore two regions were collected for the spectra ranging from 590 to 1760 cm^{-1}. The first region ranges from 590 to 1230 cm^{-1} and the second region from 1130 to 1760 cm^{-1}. The overlapping part of 100 cm^{-1} was used to enable the Software package to properly connect the two spectra after the spectral treatment (for details see chapter 4.4.1.).

Intensity of Laser Beam. The intensity of the laser beam at 488 nm was usually set to 100mW at sample space to ensure that the sample will not be damaged during the measurement. In case of Sac7d which is a very stable protein and its complex with DNA, the laser power was set to 200 mW at sample space. To check whether the laser power caused any damage to the sample, the spectra obtained during the time course of the measurement were always compared before averaging (see below). The laser power was controlled by a laser-power-meter Type 200 from Coherent (Santa Clara, CA, USA).

Measurement Time. Typically, 15 spectra, each measured for exactly 120 s, were accumulated and averaged to produce the spectra shown in Chapter 5. Samples of Sac7d and Arc proteins were exposed for 50 min each to get the two spectral regions that were measured for the gluing of the full spectra shown in the figures. Thus, 10 spectra, each accumulated for 300 s, were collected and then averaged. To exclude all possible drifts of the wavenumber scale during the measurements, a calibration spectrum was collected after each 120 s (300 s) accumulation step of sample spectra.

Calibration. For the comparison of Raman spectra and for the calculation of difference spectra, the accuracy of the peak positions is crucial. Several factors can influence the wavenumber accuracy; especially moving of the grating of the monochromator could be a source of minor shifts which cannot be avoided by standard calibration procedures. To guarantee a high accuracy of the calibration it is necessary to collect a calibration spectrum with sharp lines of exactly known peak positions immediately after each sample measurement. A neon glow lamp was used as an emission source and provides an ideal calibration spectrum. It is composed of many lines suitable for calibration in the 489 – 640 nm region. Argon or mercury might be present as contaminations in some lamp fillings and provide additional lines which are useful for calibration purposes.

The calibration of the sample spectrum is performed in four steps by our program BERKAL1: (i) determination of the accurate peak positions in the neon glow lamp calibration spectrum; (ii) assignment of these peaks to the tabulated lines of neon (argon, mercury); (iii) least-squares fit of wavenumber versus pixel position for the identified lines; (iv) conversion of the sample spectrum pixel scale to wavenumber scale.

Within the first step, the program finds the positions of all peaks in the neon glow lamp calibration spectrum which are significantly higher than the noise (typically about 50 peaks). Then, these peak positions are refined up to subpixel resolution by Gaussian curve fitting. In the second step, the program assigns the most intensive peaks of the calibration

spectrum to the tabulated lines. The program contains a table of suitable selected spectral lines with their wavelengths and positions on the pixel scale of a virtual CCD detector with 10,300 pixels. The calibration spectra were collected in advance and all peaks were assigned. After that, the data have been built into the calibration program. The pixel peak positions only and not the peak intensities are used for the assignments. After step (ii), the program has information about the pixel positions and corresponding wavenumbers of approximately ten peaks (where wavenumber is the Raman shift between the wavelength of the neon line and the laser excitation line). The pixel-wavenumber data pairs are then fitted by a cubic polynomial that is used in the final step for the conversion of the sample spectrum from the pixel scale into the precise wavenumber scale.

4.3.2. Circular Dichroism (CD), Fluorescence, and Concentration Measurements

CD spectra in the far ultraviolet region were obtained with a Jasco-J720 (Japan Spectroscopic Co., Tokyo, Japan) spectropolarimeter using 0.001 cm path length quartz cuvettes at 23 °C. 5 spectra, each collected for two minutes with 0.2 nm steps in the region between 320 and 203 nm, were averaged to produce spectra shown in Figure 5.2.

Tryptophan fluorescence spectra were obtained at 23°C with a Jasco-FP6500 (Japan Spectroscopic Co., Tokyo, Japan) spectrofluorimeter at an excitation wavelength of 280 nm, and with 1 nm and 5 nm bandwidths for the excitation and emission monochromators, respectively. Each spectrum shown in Figure 5.2 was collected in the region between 280 and 450 nm. The monochromator steps were set to 0.1 nm and each point of the spectra was accumulated for 0.5 s.

The concentration of the samples was determined by measurement of the absorption spectra on the Uvikon 930 absorption-spectrometer (Kontron Instruments, Neufahrn, Germany) at 23 °C.

4.4 Interpretation of Raman Spectra

Raman spectroscopy belongs to a broad spectrum of techniques which can be applied to investigate structural features of proteins, nucleic acids and their nucleoprotein assemblies or complexes. A principal advantage of this method is that it can be applied to virtually any sample morphology. For biological specimens, this includes aqueous and non-aqueous solutions, suspensions, precipitates, gels, liquid crystals, single crystals, and

polycrystalline and amorphous solids. Here, the basic assignment and the structural interpretation of Raman bands of proteins and nucleic acids are given.

4.4.1. Evaluation of Raman Spectra

Over 30 Raman bands can be found in the Raman spectra of both proteins and nucleic acids in the spectral region 600 to 1750 cm^{-1}. Most of them have been assigned in the last 35-40 years by the analysis of model substances or samples with known structures. However, there still exist large gaps in the available knowledge that do not allow the extraction of the full information content of Raman spectra.

Before the evaluation of the spectrum can be started the buffer and background spectra must be eliminated from the collected spectrum.

After the spectrum calibration (for details see chapter 4.3.1.), the normalized buffer spectrum was subtracted. The normalization of the buffer spectrum was done according to TRIS peaks at 1470, 1063, and 759 cm^{-1}. The strong water band near 1640 cm^{-1} overlaps with protein amide I and DNA guanine and thymine bands and therefore it was rejected from the normalization procedure. One of the disadvantages of Raman spectroscopy is that the Raman effect of inelastic light scattering is very weak compared to other light absorption and emission processes. Visible laser radiation (here 488 nm) is normally employed to excite the Raman spectrum of DNA or protein. Although proteins and DNA do not absorb in the visible wavelength region, extreme care and effort must be devoted to the elimination of even minute traces ($1:10^6$) of fluorescent impurities or other contaminations that absorb visible radiation. The background may easily overlap the Raman spectrum of protein or DNA because of the high quantum yield of fluorescence. Therefore, samples for Raman measurements need special care during purification and handling procedures. Residual fluorescence was reduced by bleaching in the laser beam before collection of the Raman spectrum. After buffer subtraction, the fluorescence background was removed. For this purpose the fluorescence background was approximated by a polynomial curve.

4.4.2. Raman Spectra of Proteins

The bands in the Raman spectrum of protein are caused by vibrations of peptide backbone and amino acid side chains. The amide bands reflect the secondary structure of the protein, whereas side chain bands carry information about the local environment of the corresponding groups.

Amide Bands and Secondary Structure. The vibrational modes of amide I, II, and III are illustrated in Figure 4.3. The frequencies of these modes reflect the structure of the main polypeptide chain. Typical frequencies for α-helix, β-sheet, and irregular structures are summarized in Table 4.1. The frequency of the respective secondary structure element is not very strict, because it is dependent on the strength of the hydrogen bond at the C=O···N–H moiety (–CONH–).

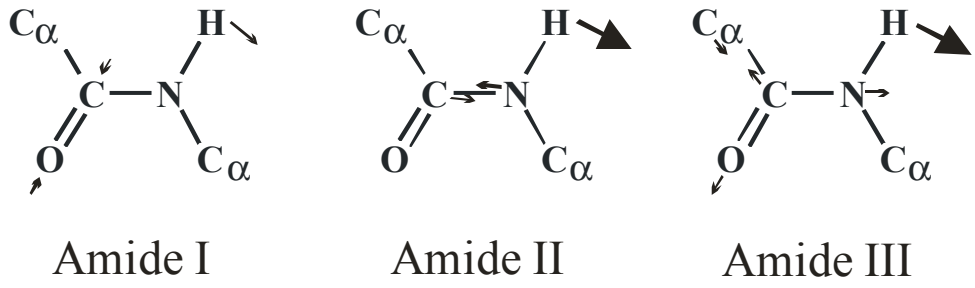

Figure 4.3: Schematic representation of vibrational modes of amide I, amide II, and amide III (*77*).

Table 4.1: Raman Markers of Amide I and Amide III bands in Proteins[a]				
Secondary structure	Amide I (H_2O)	Amide I' (D_2O)	Amide III (H_2O)	Amide III' (D_2O)
β-sheet	1665-1680	1655-1670	1230-1240	970-1000
α-helix	1645-1660	1635-1645	1260-1300	950-960
unordered	1660-1665	1655-1660	1240-1250	900-930

[a] Frequencies in cm^{-1} units were determined from Raman spectra of proteins of known secondary structure (*78-80*).

The amide I band is assigned to mainly C=O stretching mode, while the amide III band is due to C–N stretching mixed with N–H bending. Deuteration changes the frequencies of those bands. Due to the mixing with N–H bend, the amide III band disappears when –CONH– is deuterated, and the amide I bands slightly shifts to lower wavenumbers. Amide III' bands of deuterated proteins appear at more than 250 cm^{-1} smaller wavenumbers compared to bands of non-deuterated samples. The amide II mode, which is an N–H bend coupled with C–N stretch, is usually very weak and cannot be identified in Raman spectra. However, after the H–D exchange, the band slightly downshifts and becomes very intense.

Results of Raman spectroscopic determination of secondary structure elements from Raman intensities of the amide I and III bands are based of X-ray crystallographic structural data and are in general agreement with those of determined by CD spectroscopy (*81*).

Amino Acids. Very characteristic Raman bands are caused by vibrations of aromatic side chains. These three amino acids are illustrated in Figure 4.4 and their Raman markers will be described in the following. The band positions may vary up to 5 cm^{-1} in the Raman spectra of proteins.

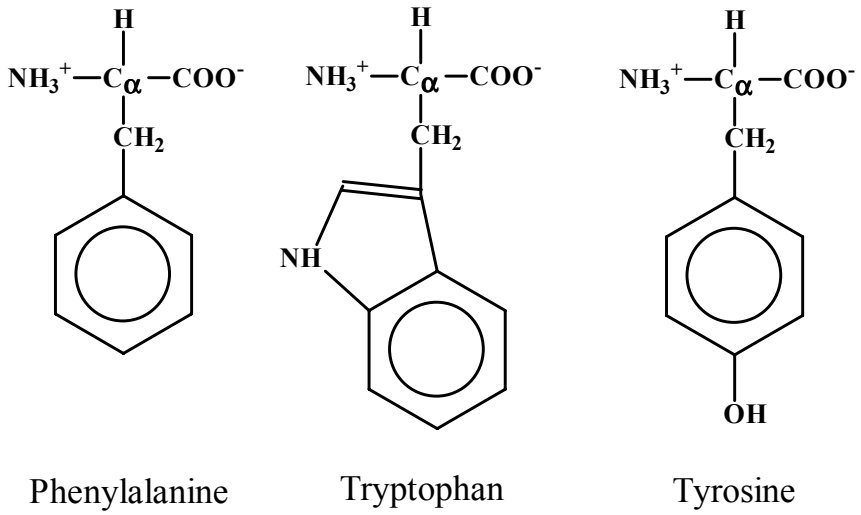

Figure 4.4: Structural diagrams of aromatic amino acids phenylalanine, tryptophan, and tyrosine.

Tyrosine. Raman bands at 645, 830, 850, 1175, 1205, 1260, 1605, and 1615 cm^{-1} are assigned to tyrosine aromatic side chain. These bands show only minor or no shift upon H–D exchange. The most important bands are the so called tyrosine doublet near 830 and 850 cm^{-1}. The relative intensity of the two bands is very sensitive to the Tyr environment (*82*). They are caused by Fermi resonance between the in-plane breathing mode of the phenol ring and an overtone of out-of-plane deformation mode (*82*). The intensities of these two bands depend on the hydrogen bonding condition of the phenol side chain. The relative intensity (I_{850}/I_{830}) ranges from 6.7 to 0.3 (*83*). A relative intensity value of 6.7 corresponds to non-hydrogen bonded tyrosine. At a value of 2.5 the OH group of tyrosine is a strong hydrogen bond acceptor, whereas a value of 0.3 corresponds to tyrosine as a donor of a strong hydrogen bond. A value of 1.25 shows that the OH group serves both as an acceptor and a donor of a hydrogen bond. When a given protein contains a single Tyr residue, the relative intensity of the doublet provides fairly precise information about the Tyr environment, but for proteins with more than one Tyr residue the Raman information shows always an average over all Tyr residues.

Tryptophan. 18 bands are assigned to the aromatic amino acid tryptophan. These bands are labeled from W1 to W18 in the region 1700-700 cm^{-1}. The most important are: 1615 (W1), 1585 (W2), 1550 (W3), 1435 (W6), 1360 (W7), 1340 (W8), 1010 (W16), 880

(W17), 760 (W18). All these vibrational modes can be assigned to vibrations of the indole ring. Vibrations W4 and W5 as well as W7-W15 are very weak and moreover, they overlap with intense bands of aliphatic side chains and amide III bands. In D_2O, one more band appears near 1380 cm^{-1}. The bands at 1550, 1360, 1340, 1010, 880, and 760 cm^{-1} are very sensitive to the tryptophan surroundings.

The Trp band near 1549 cm^{-1} (W3) assumes wavenumber values between 1542 and 1557 cm^{-1} depending on the absolute value of the $C_\alpha C_\beta$-C_3C_2 torsion angle $|\chi^{2,1}|$ which usually varies between 60° and 120°. According to ref 25 the torsion angle $|\chi^{2,1}|$ can be calculated from experimentally determined wavenumber X of the W3 mode using the empirical equation:

$$X = 1542 + 6.7(\cos 3|\chi^{2,1}| + 1)^{1.2}. \qquad (4.1)$$

For model compounds in solution, the components of the Fermi doublet of Trp were found at about 1360 (W7) and 1340 cm^{-1} (W8). The intensity ratio $R=I_{1360}/I_{1340}$ serves as a hydrophobicity marker. The 1360 cm^{-1} component of the doublet is strong in hydrophobic solvents whereas in hydrophilic environment the 1340 cm^{-1} component is stronger. R is below 0.9 for hydrophilic solvents and higher than 1.1 for hydrophobic solvents (*84*).

The 1010 (W16) band is sensitive to the strength of van der Waals interactions of the phenyl ring of Trp with surrounding residues (see Chapters 5.3 and 5.4). Wavenumbers near or below 1010 cm^{-1} indicate weak or no van der Waals interactions, whereas increasing wavenumbers near 1012 or higher reflect stronger van der Waals interactions.

For the W17 mode, the frequency varies between 883 and 871 cm^{-1}; without H-bonding at the N1 site of Trp this band is located at 883 cm^{-1}, and with strong H-bonding the band shifts to 871 cm^{-1} (*84*).

The very strong Trp band near 761 cm^{-1} (W18 mode) is a sensitive marker to the hydrophobicity of the indole ring environment (*85*). A Trp side chain in hydrophilic environment gives rise to a very strong band while in hydrophobic environment the band becomes weaker (*85*).

Phenylalanine. The aromatic amino acid phenylalanine shows Raman bands near 620, 1003, 1030, 1210, 1585, and 1610 cm^{-1}. The very intense band at 1003 cm^{-1} is not sensitive to conformational changes of protein and therefore can be used for normalization of the Raman spectra of protein (*86*).

Other amino acids. Bands caused by S–H stretching vibrations of cysteine can be found between 2530 and 2550 cm^{-1}. Disulfide bridges, if present, play a critical role in

maintaining of the tertiary structure of proteins. The S–S stretching frequency varies from 510 to 540 cm^{-1} depending on the conformation of –C–S–S–C–. The A band in the region 630-670 cm^{-1} is assigned to stretching vibrations of –C–S– in the *gauche*-conformation, the band is localized between 700 and 745 cm^{-1} in case of the *trans*-conformation of –C–S–. Several bands are assigned to vibrations of CH_3, CH_2, and CH groups. The most intense bands are the one of CH_2 at 1312 and 1342 cm^{-1} caused by twisting and wagging, the one at 1447 cm^{-1} caused by CH_2 scissoring, and a band near 1462 cm^{-1} of the the CH_3 asymmetric vibration. A band found near 1400 cm^{-1} belongs to carboxyl group vibrations. Other examples are listed in Table 5.2.

4.4.3. Raman Spectra of Nucleic Acids

The positions and intensities of several marker bands in a Raman spectrum provide information about the conformation of an unknown DNA. The marker bands can be divided into two classes: (i) marker bands of the nucleoside conformation and (ii) marker bands of the phosphate backbone. The positions of the marker bands were derived from Raman spectra of crystals, fibers, and solutions of DNA or RNA of known structures that were used as reference molecules. Usually the structures of reference molecules were determined by X-ray crystallography and/or NMR spectroscopy.

In vivo DNA is usually structured in B-form. B-DNA is observed in low ionic strength aqueous solutions and in fibers or films exposed to high relative humidities. A-DNA is stabilized in low water activity conditions, for instance in water-ethanol solutions or in fibers or films exposed to below 76% relative humidity. It is possible to transform B- to A-DNA by changing the surroundings of the double helix. The main differences between structures going from B- to A-form are: (i) changes in the conformation of the DNA backbone (ii) changes in the sugar pucker from C2´-endo (S-type) to C3´-endo (N-type). The left-handed double helical Z conformation of DNA can be obtained in solution by interaction with transition metal ions in low water activity conditions. The sugar puckers alternate in Z conformation between C3´-endo/syn for purines and C2´-endo/anti for pyrimidines.

The deoxyribose ring is in general not in plane. Four atoms of the ring build a plane envelop-form and the fifth atom hangs out of plane by ~ 0.5 Å. If the out-of-plane atom points to the same direction as the C5´atom, the conformation is called *endo*. The conformation is called *exo* when the C5´atom is located in the opposite direction.

Bases may be orientated in syn- or anti-conformations relative to the C1′–N glycosidic bond. In the anti-conformation, the bases are orientated out of the sugar ring, whereas in the syn-conformation the bases point toward the deoxyribose rings. Other details of the DNA structures can be found in ref 87.

The conformation of the furanose rings and the orientation of the glycosidic bond are reflected by specific Raman markers, which are summarized in Table 4.2. Table 4.3 indicates characteristic Raman marker positions of different conformations of the DNA backbone.

Table 4.2: Raman Markers of Nucleoside Conformation in Nucleic Acids[a]

Base	C3′-endo/anti	C2′-endo/anti	C1′-exo/anti	C3′-endo/syn	C2′-endo/syn
G	664 ± 2[b]	682 ± 2	670 ± 2	625 ± 3	671 ± 2
	1318 ± 2	1333 ± 3[c]	1343 ± 2	1316 ± 2	1316 ± 2
A	644 ± 4	663 ± 2[d]		624 ± 3	
	1335 ± 2	1339 ± 2		1360 ± 5	
C	780 ± 2	782 ± 2		784 ± 2	
	1252 ± 2	1255 ± 5		1265 ± 2	
T	668 ± 2[e]	668 ± 2		660 ± 5	677 ± 2
	745 ± 2[f]	748 ± 2		745 ± 5[f]	737 ± 2
	777 ± 2	790 ± 3			
	1239 ± 2	1208 ± 2			

[a] Frequencies in cm^{-1} units were determined from Raman spectra of DNA and RNA crystals and fibers of known structure (Adopted from ref 88 and 89).
[b] Observed at 668 ± 1 in structures containing rG.
[c] A weak companion line near 1316 cm^{-1} is also observed in B-DNA structures.
[d] Very low intensity compared to 664 and 668 cm^{-1} lines of C2′-*endo/anti* dG and C2′-*endo/anti* dT, respectively.
[e] Very low intensity compared to 668 cm^{-1} line of C2′-*endo* conformer.
[f] Very low intensity compared to 748 cm^{-1} line of C2′-*endo* conformer.

Table 4.3: Raman Markers of Nucleoside Conformation in Nucleic Acids[a]

Group	A-DNA	B-DNA	Z-DNA
O-P-O	706 ± 5	790 ± 5	745 ± 3
	807 ± 3[b]	828 ± 2 (GC)	
		835 ± 2 (GC + AT)	
		839 ± 2 (AT)	
PO_2^-	1099 ± 1	1092 ± 1	1095 ± 2
CH_2	1418 ± 2	1422 ± 2	1425 ± 2

[a] Frequencies in cm^{-1} units were determined from Raman spectra of DNA and RNA crystals and fibers of known structure (Adopted from ref 88 and 89).
[b] This vibration occurs at 813 ± 2 cm^{-1} in A-RNA structures. A very weak line also occurs at approximately 810 cm^{-1} in Z-DNA structures.

4.4.4. Raman Spectra of Protein–DNA Complexes

The evaluation of the Raman spectra of protein–DNA complexes is based on the comparison with the Raman spectra of particular components of the complexes. Normalization of the spectra is a very important step in data evaluation to ensure equal amounts of components and complex in the spectra that have to be compared. For normalization of the protein spectrum, the phenyl breathing vibration of phenylalanine at 1003 cm^{-1} is suitable, because it is invariant to complex formation (*86*). If there is no phenylalanine in the protein sequence the CH_2 breathing vibration at 1447 cm^{-1} may be used. DNA is commonly normalized to the phosphate band at 1092 cm^{-1}. The intensity of the phosphate band is usually independent of nucleic acid and protein interactions (*90*).

Differences between the Raman spectrum of a complex and the calculated sum of component spectra reflect spectral changes that result from complex formation. The difference spectra contain information about conformational changes and interactions of DNA and protein in the complex. The difference spectrum is normally calculated in several steps. First, both component spectra must be normalized according to rules mentioned above. Then, the spectra of DNA and protein are subtracted followed by subtraction of the buffer spectrum. Finally, the fluorescence background is removed. Difference bands are considered as significant when the following criteria are fulfilled:

(i) The intensity of the difference band is at least two times higher than the signal-to-noise ratio.

(ii) The difference band reflects an intensity change of at least 5% of its parent band.

(iii) Corresponding difference bands were obtained from spectra measured in H_2O and D_2O buffers.